Available online at www.sciencedirect.com
ScienceDirect
Ceramics International 38 (2012) 77–84
CERAMICS INTERNATIONAL
www.elsevier.com/locate/ceramint

Porosity control of cold consolidated geomaterial foam: Temperature effect

Joseph Henon, Arnaud Alzina, Joseph Absi, David Stanley Smith, Sylvie Rossignol *

Centre Européen de la Céramique, Groupe d'Etude des Matériaux Hétérogènes, Ecole Nationale Supérieure de Céramique Industrielle, 12, rue atlantis, 87068 Limoges cedex, France

Received 3 May 2011; received in revised form 17 June 2011; accepted 17 June 2011
Available online 24th June 2011

Abstract

Porous K-geopolymers with mutli-scale porosity were synthetized, based on the production of molecular hydrogen due to the oxidation of free silicon associated with polycondensation reactions. The various drying steps at low temperatures influencing the foams morphology were evaluated in function of parameters like mass effect, mold dimensions and drying cycles. The results obtained evidenced the possibility to perform reproducible foams with a control of their porosity. These foams are in agreement with the environmental demand with their recycling properties and their low cost of production due to the cheap materials used and the low temperature of synthesis. Some other advantages like their fire resistance, acid/base resistance, their good mechanical properties and their good thermal conductivity is a good point for future applications. As an example a homogeneous foam with a pore size of 1.5 mm at 50 °C (9 days for an achieved drying but consolidated before) can be prepared. Moreover the porosity can be controlled with various temperature cycles decreasing the time of synthesis. From the cycles tested (70–55 °C and 70–23 °C), some homogeneous samples were obtained with pores sizes varying from 0.5 to 1.5 mm. Then the work was extended to larger surfaces exchange, what evidences the importance of drying and mass effects upon the porosity as well as the mechanical properties of the mold used during synthesis.

Keywords: Porous material; Geopolymer; Foam; Microstructure; Temperature cycle

1. Introduction

There are many applications [1,2] for porous ceramics related to their properties of high permeability, low bulk density, high surface area, and low thermal conductivity. Each of these properties is linked to the solid part chemical composition and to the final pore volume fraction and structure in term of morphology, size and connectivity. In this respect processing has an important role. Many methods have been explored to synthesize reproducible foams with a homogeneous pore characteristics, such as (PU) Polyurethane replicas or an equivalent sponge/organic substrate burned after impregnation [3], addition and sintering of calibrated pore forming agents [4], gel casting [5,6], and direct foaming [7]. Generally, the pores are created either with a dispersion of gas inside a slurry (emulsions), either with a calibrated skull, or a calibrated pore forming agent eliminated inside a solid matrix. When the gaseous method is chosen, as it is in this work, it is difficult to control the pore size distribution and the viscosity, the surface tension and the pressures [8] are essential parameters to control. In this case, foam has been defined by Breward [9] as a ''gas–liquid mixture in which the volume fraction of the liquid phase is small''. Foams can be wet or dry, depending on the proportion of liquid contained in them. In wet foam the bubbles are approximately spherical, while in dried foam these are polyhedral.

Additives called surfactants (or tensioactives) can be used to control surface tension [10,11] and repartition of particles or bubbles. To resume, these additives can be ionic or non-ionic and are some amphiphilic: having a hydrophilic part and a hydrophobic part to the same molecule. These specific properties create a better affinity with the interfaces where they adsorb on, reducing the interface surface tension. Moreover at sufficiency high bulk concentration they can form structures in solution with self-assembly capability [9]. The inconvenience is that these additives are an additional cost and could be a source of CO_2 emission.

Due to questions related to the effect of gas emissions for the environment, new materials have been sought as an alternative

* Corresponding author.
E-mail address: sylvie.rossignol@unilim.fr (S. Rossignol).

0272-8842/$36.00
doi:10.1016/j.ceramint.2011.06.040

to cement. Geopolymers are good candidates [12]. At low temperature (<100 °C) their manufacturing emits six times less CO_2 than standard cements [13]. Previous work in our laboratory has demonstrated how to synthesize a geomaterial from clay, alkali silicate and alkali hydroxide in an aqueous environment [14].

The addition of silica fume as a pore forming agent yields a final solid inorganic foam with a geopolymer matrix [15]. An interesting aspect of this foam is its potential for insulation due to a low value of thermal conductivity. The mechanisms involved in the formation of the porous structure are based on the competition between the formation of molecular hydrogen gas due to the oxidation of free silicon element (Eq. (1)), contained in the silica fume used, and the polycondensation reactions [12] responsible for hardening. Under basic conditions, free silicon is oxidized by water, causing the formation of hydrogen (Eq. (1)). The presence of hydrogen gas has already been verified by thermal analysis coupled with mass spectrometry. Then, the dissolution of raw materials leads to the formation of a chemical gel. The influence of the silica fume and its silicon content on the final volume of the foam was evidenced in previous work on the laboratory [15]. Consequently the gas bubbles are trapped inside the material.

$$4H_2O + Si \xrightarrow{\text{basic media}} 2\vec{H}_2 + Si(OH)_4 \quad (1)$$

The kinetics of the reaction described in Eq. (1) and the polycondensation reaction depend on the different concentrations of species, the temperature of the system and the pressures [16]. The polycondensation reaction results in the hardening of the material (and then on the viscosity) whereas the kinetic of the gassing reaction influences the quantity of gas produced. The rheological behavior of gas bubbles in a liquid [8–17] or gas bubbles in a suspension (liquid–solid–gas system) with particles [18] and the evolution of aqueous foams is well described in the literature. Considering a curved interface separating two media, Young and Laplace have established a relation between the curvature of the interface and the difference of pressure between each side of the interface. If the bubbles do not burst two phenomena are responsible for its evolution: the drainage and the maturation. Drainage is controlled by capillarity and gravity. The capillarity induces a fluid displacement from the lamellae to the Plateau borders [9]. The influence of gravity depends on the capability of interface slipping [19]. The maturation corresponds to gas diffusion from bubbles leading to pore coalescence. The fact that the foam is prepared in an open system, where thermal and mass exchanges occur between the air and the foam, implies that the drying aspect, associated with the consolidation, is important for the drainage of the liquid [8–17]. Capillarity will also affect particle arrangement [18]. Finally, the type of mold used and its characteristics in term of shape, surface, and mechanical behavior should be taken into account.

To find an application in building construction, the problematic is to create a porous isolating mineral material with a multi-scale porosity, with a low environmental impact processing. For all its advantages, the geopolymer foams offer a good issue since these can, be synthesized without additives with a low processing temperature and with good recycling properties. The purpose of this study is to control the porosity, through an understanding of the roles of the viscosity and the polycondensation reactions. These are influenced by the experimental conditions. The temperature of drying steps and the sample environment during this process were tested to establish the best conditions to control the foam porosity.

2. Experimental procedure

2.1. Preparation of geopolymer foams

2.1.1. Raw materials

The silicate solution used in this work is a commercial potassium silicate (Prolabo) with a moisture content of 76%, a ratio of Si/K = 1.7 and a density equal to 1.33. KOH pellets (Alfa Aesar) are 85% pure. The silica fume (Ferropem[1] Company, D_{50} = 0.15 μm, S_{BET} = 30.4 $m^2\ g^{-1}$) is used as a gas forming agent (containing 0.7% of free silicon for hydrogen gas production) and to enrich the slurry with an increase amount of Si. The kaolin (AGS[2] (France), D_{50} = 5 μm, S_{BET} = 17 $m^2\ g^{-1}$) has been dehydroxylated at 750 °C.

2.1.2. Preparation protocol

The protocol of preparation is described in Fig. 1 following Prud'homme et al. [15]. Potassium hydroxide pellets are placed in a solution of potassium silicate which is agitated for 1 min in a Teflon mold with a magnetic stirrer at a rate of 650 rpm, so that the pellets are totally dissolved inside the solution. Then the metakaolin powder and silica fume are added and mixed for 3 min at a higher agitation speed of 850 rpm. After agitation, the slurry is poured into cylindrical polypropylene or polystyrene molds (Φ = 1.4, 3.3 or 5 cm, height = 7 cm) placed in an oven at a temperature T for a time t.

2.1.3. Nomenclature of sample

The nomenclature of sample is given by: ${}^{\Phi}{}_{m/m_0}F^{t_1-T_1}$.

A sample, with a mass m introduced in a cylindrical mold with a diameter Φ at a first temperature T_1 during t_1 hours and a final temperature T_2 for t_2. m_0 is the standard mass of sample obtained from the standard composition: 20 wt% metakaolin, 18 wt% silica fume, 51 wt% silicate and 11 wt% KOH. The different samples are presented in Table 1. For example, the nomenclature of a sample elaborated with a mass m_0 g of potassium foam poured into a mold with a 3 cm diameter, dried at 55 °C after a 1 h step at 70 °C will be written ${}^{3}{}_{1}F^{1-70}{}_{55}$.

2.2. Characterization

2.2.1. Gravimetry and volume expansion

Sample gravimetry was made by measuring its weight loss at different times until the foam was consolidated meaning no mass variation. At the same time the volume of foam was

[1] Ferropem: 517 avenue de la Boisse 73025 Chambery Cedex, France.
[2] AGS, 17270 Clerac, France.

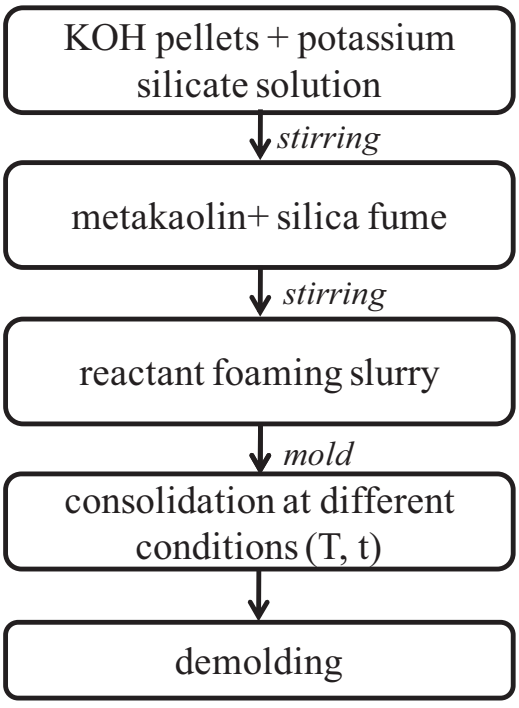

Fig. 1. Schematic diagram of porous geopolymer processing at low temperature.

measured. The resulting ratio between the foam volume at instant t to the initial volume of liquid introduced is named the volume expansion noted $E_v(t)$.

2.2.2. Thermal analysis

Differential thermal analysis (DTA) and thermo gravimetric analysis (TGA) was performed to characterize the sample $^{3.3}{}_1F^{70}$ when totally dried. This experiment was carried out in a Pt crucible between 30 and 1200 °C with a 10 °C min^{-1} heating ramp in dry air conditions using a Setaram Setsys evolution apparatus.

2.2.3. Density measurement

The bulk densities of foams are given by the ratio between the mass of a parallelepiped of foam divided by its apparent volume. For a foam, the bulk density was measured at different heights. The density of the matrix is determined with an Accupyc 1330 (Micrometrics) helium pycnometer. The sample was crushed and passed through a 63 μm sieve before measurement. This was repeated 4 times per sample and the mean value was taken.

2.2.4. Microstructure analysis with microscopy

The microstructure was studied using both a Nikon eclipse 50i optical and a Cambridge Stereoscan S260 scanning electron microscope. The pore size distribution was evaluated from the analysis of each sample cut at different heights using the Image J software. As the pores are spherical, the mean pore diameter Γ_v [20,21] was calculated for each cut as follows:

$$\Gamma_v = \frac{\sum_{i=0}^{n} n_i {d_i}^4}{\sum_{i=0}^{n} n_i {d_i}^3} \quad (2)$$

where d_i = pore diameter for class i, n_i/n = number of pore inside the class i/total number of pores.

3. Results and discussion

The experimental results in term of volume expansion (E_v) and mean pore diameter (Γ_v) are given in Table 2 for all samples after synthesis (total weight loss of 35.5%) as well as the ratio $\varnothing/H$, where $\varnothing$ is the diameter of the mold and H is the height of mixture poured into the mold.

Table 1
Samples and their nomenclature (PP: polypropylene, PS: polystyrene).

Mold		Temperature (°C)		m/m$_0$	Drying times		Nomenclature
Ø (cm)	Nature	T_1	T_2		t_1 (h)	t_2 (days)	
1.4	PS	70	70	0.08	0	7	$^{1.4}{}_{0.08}F^{70}$
				0.12			$^{1.4}{}_{0.12}F^{70}$
				0.18			$^{1.4}{}_{0.18}F^{70}$
3.3	PS	70	70	0.27	0	7	$^{3.3}{}_{0.27}F^{70}$
	PS			1.00			$^{3.3}{}_{1}F^{70}$
	PP			1.00			$^{3.3PP}{}_{1}F^{70}$
3.3	PS	70	55	1.00	0.5	9	$^{3.3}{}_{1}F^{0.5\text{-}70}{}_{55}$
				1.00	1.0	9	$^{3.3}{}_{1}F^{1\text{-}70}{}_{55}$
				1.00	1.5	9	$^{3.3}{}_{1}F^{1.5\text{-}70}{}_{55}$
				1.00	2.0	9	$^{3.3}{}_{1}F^{2\text{-}70}{}_{55}$
		55	55	1.00	0	9	$^{3.3}{}_{1}F^{55}$
		70	23	1.00	0.5	20	$^{3.3}{}_{1}F^{0.5\text{-}70}{}_{23}$
				1.00	1.0	20	$^{3.3}{}_{1}F^{1\text{-}70}{}_{23}$
				1.00	1.5	20	$^{3.3}{}_{1}F^{1.5\text{-}70}{}_{23}$
				1.00	2.0	20	$^{3.3}{}_{1}F^{2\text{-}70}{}_{23}$
		23	23	1.00	0	20	$^{3.3}{}_{1}F^{23}$
5.0	PP	70	70	1.00	0	7	$^{5}{}_{1}F^{70}$
				1.50			$^{5}{}_{1.5}F^{70}$
				2.30			$^{5}{}_{2.3}F^{70}$
				3.45			$^{5}{}_{3.45}F^{70}$

Table 2
Various data of potassium foam samples after synthesis (PP: polypropylene, PS: polystyrene).

Sample	Mold	Ø/H	$E_v \pm 7\%$	$<\Gamma_v> \pm 5\%$ (mm)
$^{3.3}{}_{1}F^{70}$	PS	1.5	2.80	3.70
$^{3.3}{}_{1}F^{55}$	PS	1.5	2.25	1.95
$^{3.3}{}_{1}F^{23}$	PS	1.5	1.65	1.20
$^{3.3}{}_{1}F^{0.5\text{-}70}{}_{55}$	PS	1.5	2.05	1.50
$^{3.3}{}_{1}F^{1\text{-}70}{}_{55}$	PS	1.5	2.00	1.35
$^{3.3}{}_{1}F^{1.5\text{-}70}{}_{55}$	PS	1.5	2.05	1.20
$^{3.3}{}_{1}F^{2\text{-}70}{}_{55}$	PS	1.5	2.10	1.45
$^{3.3}{}_{1}F^{0.5\text{-}70}{}_{23}$	PS	1.5	1.44	0.85
$^{3.3}{}_{1}F^{1\text{-}70}{}_{23}$	PS	1.5	1.40	0.55
$^{3.3}{}_{1}F^{1.5\text{-}70}{}_{23}$	PS	1.5	1.55	0.60
$^{3.3}{}_{1}F^{2\text{-}70}{}_{23}$	PS	1.5	1.60	0.70
$^{1.4}{}_{0.08}F^{70}$	PS	1.5	2.05	0.80
$^{1.4}{}_{0.12}F^{70}$	PS	1.0	2.10	1.65
$^{1.4}{}_{0.18}F^{70}$	PS	0.7	2.15	2.50
$^{3.3}{}_{0.27}F^{70}$	PS	5.4	2.40	0.80
$^{5}{}_{1}F^{70}$	PP	5.4	2.70	0.90
$^{5}{}_{1.5}F^{70}$	PP	3.3	2.65	1.50
$^{5}{}_{2.3}F^{70}$	PP	2.3	2.60	2.70
$^{5}{}_{3.45}F^{70}$	PP	1.5	2.65	4.80
$^{3.3PS}{}_{1}F^{70}$	PS	1.5	2.80	3.70
$^{3.3PP}{}_{1}F^{70}$	PP	1.5	2.75	3.00

3.1. Behavior and characteristic at 70 °C

3.1.1. Gravimetry and volume expansion

Fig. 2 gives the volume expansion and the weight loss for a mass m_0 of foam dried at 70 °C inside a ∅ = 3.3 cm diameter polystyrene mold (sample $^{3.3}{}_{1}F^{70}$) as a function of time. The maximum volume expansion value (E_v) (Fig. 2A) is 2.8 and the final weight loss is equal to 35.5 wt% when drying is complete at this temperature. The evolution of the weight loss with time is not linear but close to a logarithmic dependence. In Fig. 2B, for the beginning of reaction, the volume expansion starts with a first stabilization step for 20 min (and a weight loss of 2%) where the E_v is stable and equal to 1.05. In fact the first bubbles appear in the slurry but the viscosity is not sufficiently high to avoid their coalescence and their release from the sample surface. After this 20 min step a crust is formed, and the growth of the foam starts. A first stable volume expansion value of 2.7 is reached after 6 h of drying but the material is not yet consolidated due to an incomplete polycondensation reaction inducing an increase of E_v. At this step, bubbles are still moving in the center of sample and demolding drives to the sagging. In order to verify the state of final drying at 70 °C and the behavior of the final foam at this temperature, differential thermal analysis was performed, Fig. 3. Three endothermic peaks are detected on the DTA curve at 120 °C, 225 °C and close to 450 °C as observed in previous work [15]. The first peak corresponds to the loss of free water. The second peak was attributed in previous work to CO_2 being given off implying the presence of some carbonate species. These result by the atmospheric carbonation of the unreacted potassium silicate and/or potassium hydroxide. The last endothermic peak at 440 °C is essentially due to the loss of structural water and the presence of zeolite phase [15]. For an initial theoretical 39 wt% of water introduced, 35.5 are lost at 70 °C during synthesis. The weight loss observed in this experiment is in agreement with the water content of the geopolymer foam.

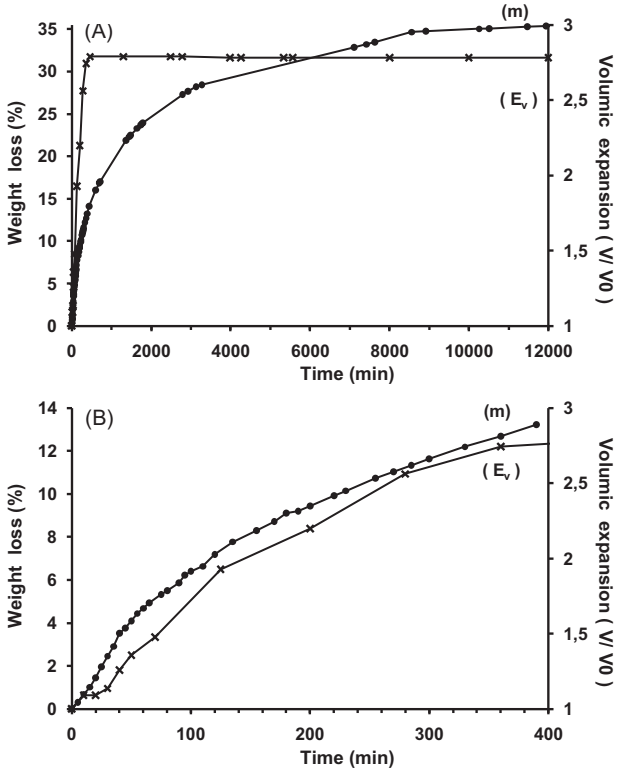

Fig. 2. Variation with time of (m) weight loss and (E_v) volume expansion values for a $^{3.3}{}_{1}F^{70}$ potassium foam (A) to a final drying and (B) at the beginning of reaction.

3.1.2. Foam morphology

Fig. 4 represents the values of Γ_v and the bulk density ρ_{bulk} of the foam at different sample heights for a totally dried sample $^{3.3}{}_{1}F^{70}$. The drying conditions at 70 °C induce variation in the pore diameters which can be separated in three zones according to the height of sample:

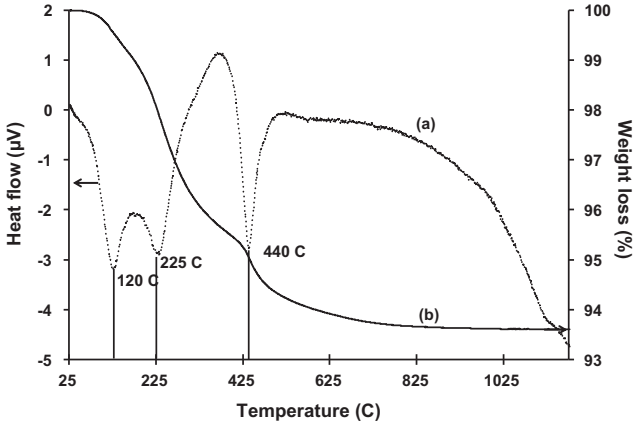

Fig. 3. (a) Heat flow and (b) weight loss of a $^{3.3}{}_{1}F^{70}$ potassium foam after total drying at 70 °C.

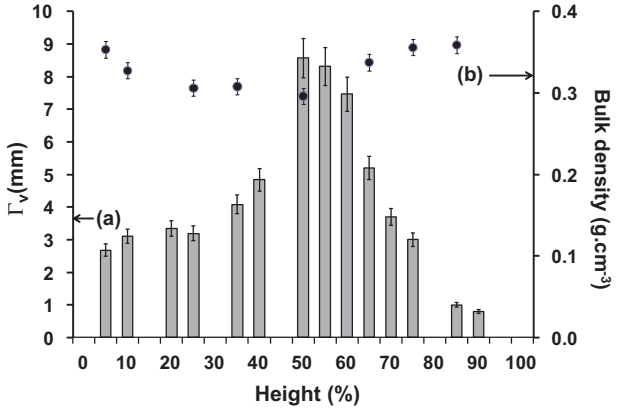

Fig. 4. Variations of (a) Γ_v and (b) bulk density for a $^{3.3}{}_1F^{70}$ sample totally dried in function of sample height.

(i) *zone 1*: from 0 to 25 height%, the mean size diameter is stable and equal to 3 mm;
(ii) *zone 2*: from 30 to 70%, the pore size is high (maximum 8 mm) and heterogeneous;
(iii) *zone 3*: above 75%, the Γ_v value decreases.

As a general rule, the values of Γ_v are high at 70 °C with a total heterogeneity. The first domain can be explained by a predominance of the gel network solidification with a coalescence of pores. In contrast, the domain 2 (middle of sample) is different because of the drying temperature which implies a competition between gel hardening and bubble gas coalescence. In fact, this competition depends also on the influence of the contact with the atmosphere since water is eliminated. Consequently, some differences can be observed along the outer limits and the core of the sample where the gas bubbles can move easily. This hypothesis is confirmed above 80% of the total height. The foam is in direct contact with the air and hardens faster due to a rapid elimination of water yielding significantly smaller pore sizes.

The ρ_{bulk} values are comprised between 0.29 and 0.36 g cm^{-3} with a mean value of 0.32 g cm^{-3}. The somewhat heterogeneous nature of the sample is reflected by fluctuations up to 10% from the mean.

3.2. Influence of temperature

3.2.1. Influence on mass loss and expansion

Fig. 5 presents both volume expansion (E_v) and weight loss values (m) as a function of time and for different drying temperatures (samples $^{3.3}{}_1F^T$). The ''Final'' value corresponds to a final equivalent weight loss of 35.5 wt% for all samples, in agreement with the initial water amount introduced. The final volume expansion values are equal to 2.80 at 70 °C, 2.25 at 55 °C and 1.65 at 23 °C and correspond to 6 h, 24 h and 20 days of drying respectively. Whatever the temperature, the allure of the $E_v(t)$ and mass(t) curves are similar. Nevertheless, the expansion is larger with temperature and the maximum value is reached faster too as the kinetics are function of the temperature [16].

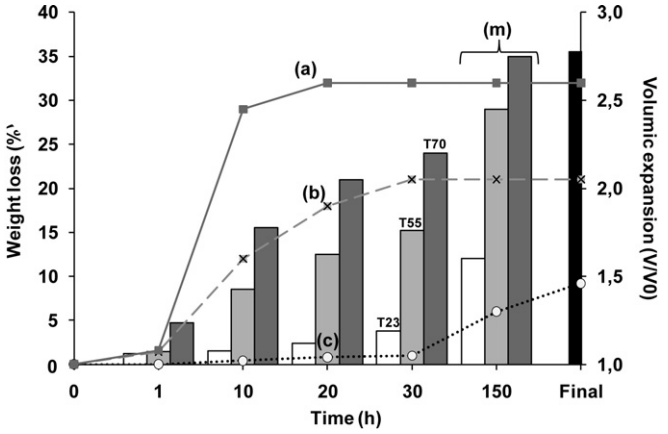

Fig. 5. Weight loss (m) and volume expansion values (a, b, c) at different times for $^{3.3}{}_1F^T$ samples for various temperatures (70 °C, 55 °C and 23 °C).

3.2.2. Influence of temperature on microstructure

Fig. 6 presents the values of Γ_v for a $^{3.3}{}_1F^T$ sample at different heights and at (a) 70 °C, (b) 55 °C, (c) 23 °C after a total weight loss for the above given time. For convenience of representation in the figure, the values of the 70 °C sample $^{3.3}{}_1F^{70}$ between 50% height and 60% height are not represented above 6 mm.

At different temperatures, the comparison of the respective Γ_v at different heights shows increasing pore size with increasing temperature. However, above 80% height, the Γ_v values are similar whatever the temperature is, as drying is predominant. Omitting this zone, at 70 °C, as it has been shown in Fig. 4, there are 3 domains of pore size from 5 mm to 8 mm and the sample is heterogeneous in the middle height. At a lower temperature of 55 °C, the Γ_v curve is linear and the Γ_v grow with height, with values varying from 1.8 mm to 2.3 mm characteristic of a quite homogeneous porosity. At 23 °C, the Γ_v values decrease linearly and these are comprised between 1.8 and 1.0 mm.

At 70 °C, the foam gel formation is very fast trapping rapidly bubbles. This is confirmed with the fact that the pore sizes at 90% height are equal to a same range of value, 0.8–0.9 mm for all temperatures. When the drying temperature decreases, both

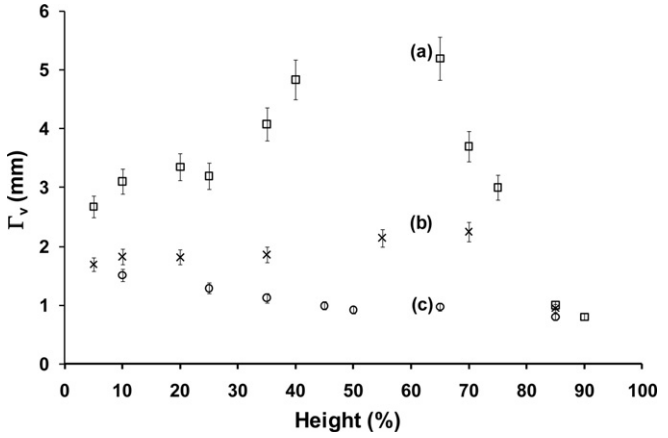

Fig. 6. Variations of Γ_v for a $^{3.3}{}_1F^T$ sample at different heights and for different temperatures (a) T = 70 °C, (b) T = 55 °C and (c) T = 23 °C.

the chemical reactions (H_2 release and polycondensation) slow down as the thermal agitation decreases. Nevertheless their kinetic evolutions with temperature [12,16] seems to be different because there is a temperature included between 45 °C and 55 °C for which one mechanism becomes predominant. This could be explained by:

(i) either a predominant polycondensation reaction responsible for trapping bubbles, inhibiting their expansion. Information on the dependence of the polycondensation kinetics with temperature is necessary to show this;
(ii) or surface tension properties as described by Laplace's laws [8], depending on pressure, the slurry viscosity and density. Again the evolution of these parameters with temperature is important. Determination of the viscosity and the density of the slurry should be made to elucidate whether this is the controlling mechanism.

As a conclusion the best drying temperature belongs to the range [45 °C, 55 °C], where Γ_v reveals the least variation as a function of height in the sample.

3.3. Porosity control with thermal cycling

As the fastest sample drying was obtained at the highest temperature but on the contrary the most homogeneous porosity was obtained for the sample synthesized at a lower temperature, it was decided to perform temperature cycling to take advantage of both aspects.

An amount of slurry (m_0) was placed into $\varnothing = 3.3$ cm diameter cylindrical polystyrene molds. Different drying steps of $t_1 = 0$, 0.5, 1, 1.5 and 2 h at 70 °C then t_2 at a lower temperature of 23 °C for the first cycle or 55 °C for the second one ($^{3.3}{}_1F^{t_1-70}$) until complete drying was achieved corresponding to a weight loss of 35.5%. The results on both final Γ_v and volume expansion are presented in Fig. 7. Each cycle results will be compared to the foam data at each reference temperature noted K_{ref}. These reference samples are the samples presented in Fig. 6 corresponding to the foams made at 70 °C, 55 °C and 23 °C (35.5% weight loss).

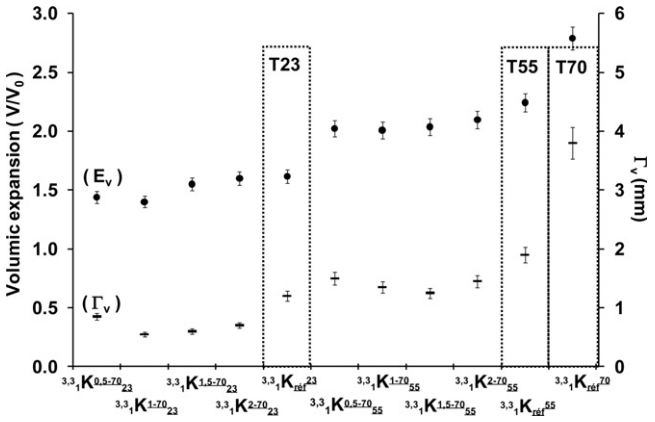

Fig. 7. Variations of E_v and Γ_v for $^{3.3}{}_1F^{t-70}{}_{55\text{ or }23}$ samples depending on the temperature cycle. The three samples T23, T55, T70 are the samples with a final dried time as reference.

For a cycle $^{3.3}{}_1F^{0.5-70}{}_{55\ °C}$ with a 0.5 h step at 70 °C, both the pore size and the volume expansion are affected. The Γ_v drops from 2.25 to 1.50 mm and the E_v from 2.8 to 2.05. Then with increasing steps (0.5 and 1 h) Γ_v decreases further (1.35 and 1.20 mm) whereas E_v is constant and is close to 2.05. For a step of 2 h, the beginning of the E_v and Γ_v increase can be observed, meaning that the previous mechanisms are predominant. In fact, the E_v and Γ_v curves are parabolic and a simple 0.5 h step at 70 °C ($^{3.3}{}_1F^{0.5-70}{}_{55\ °C}$) gives lower values in comparison to the values obtained at 70 °C. Then when the duration of 70 °C step increases both the pore size and volume expansion decrease until a 1.5 h step where minimum values are reached. Up to 1.5 h at 70 °C ($^{3.3}{}_1F^{2-70}{}_{55\ °C}$), the respective E_v and Γ_v values tend to the ones at 55 °C.

For the second cycles 70–23 °C, the behavior of porosity and volume expansion curves with these thermal cycles are similar to the one with 70–55 °C. The difference is the minimum values of Γ_v and E_v as pore size is close to 0.60 mm and the volume expansion is around 1.50.

Such thermal cycles are clearly useful concerning the porosity control. In fact the pore size diameter has a minimum value for a cycle 1 h/1 h:30 at 70 °C then 23 °C or 55 °C, keeping a volume expansion value close to those with single temperatures 23 °C or 55 °C. The consequence is an increasing pore volume fraction and a narrow pore size distribution for all heights in the sample. The drying step is reduced due to the fact that the sample was maintained at 70 °C a several time. In fact, a 1 h step at 70 °C reduces by 5% ($^{3.3}{}_1F^{1-70}{}_{55}$) to 15% ($^{3.3}{}_1F^{1-70}{}_{23}$) the total drying time obtained at the second reference temperature. However, the step at 70 °C must be limited otherwise the pore size increases as well as variation in pore size at different heights of the sample. Moreover, after 1 h at 70 °C a crust is formed and the gel foam formation becomes more significant than it is at the reference temperature. In fact at this lower temperature the crust forms later and its consolidation is slow so the flux of matter is easier. The control of the inversion of the two reactions preponderance with different cycles could explain of the curves evolution.

All these results were obtained with a constant mass introduced inside a fixed diameter of mold involving the same exchange with the atmosphere. In the next section we determine the effect of various masses introduced with various diameters to affect the reaction conditions, particularly the surface exchange.

3.4. Foam volume and surface exchange effects

Fig. 8 gives the values of volume expansion and Γ_v obtained at 70 °C with different masses introduced in different molds ($\varnothing = 1.4$ cm (PS); 3.3 cm (PS) and 5 cm (PP)). The masses introduced are chosen to have approximately equivalent final Γ_v whatever the diameter or an equivalent $\varnothing/H$ value. Between the different samples ($\neq\varnothing$) the common $\varnothing/H$ values are 1.5 and 5.4 and the common m/m_0 value is 1. However, the quantity of mass introduced is limited for a 1.4 cm diameter mold, as it is not high enough.

The volume expansion E_v and the Γ_v obtained for the $\varnothing = 1.4$ cm samples $^{1.4}{}_{0.08\rightarrow0.18}F^{70}$ (PS) with $\varnothing/H = 1.5$, 1.0,

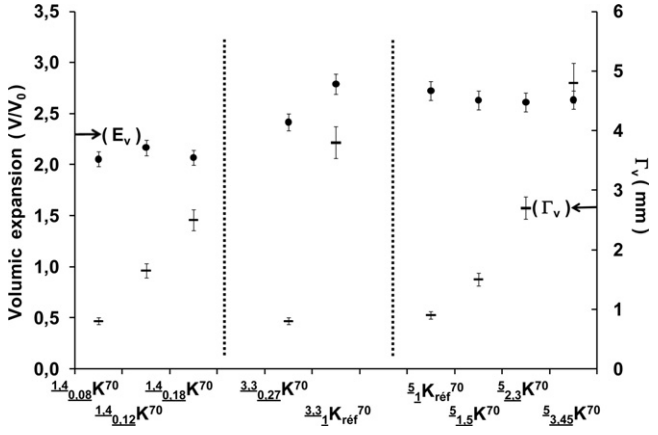

Fig. 8. Evolution of volume expansion E_v and Γ_v, for $^{\varnothing}{}_m F^{70}$ samples for different mass of foam introduced in different mold diameters $\varnothing$.

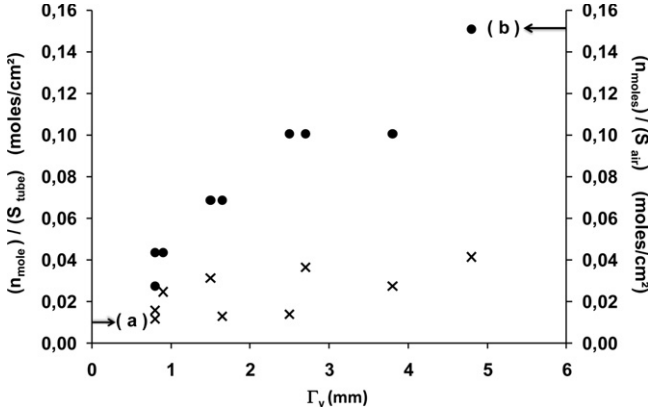

Fig. 9. Evolution of Γ_v for all samples made at 70 °C $^{\varnothing}{}_m F^{70}$ as a function of the ratios n/S_{tube} and n/S_{air}.

0.7 are respectively equal to 2.05, 2.10, 2.15 and 0.8, 1.65, 2.5 mm. So for a constant diameter $\varnothing$ = 1.4 cm, increase of the mass introduced induces a higher value of Γ_v because of the pore coalescence. Another aspect is the constant E_v whatever the mass introduced. For another diameter: $\varnothing$ = 5 cm, the samples are $^{5}{}_{1\rightarrow 3.45}F^{70}$ 5 (PP), with $\varnothing/H$ = 5.4, 3.3, 2.3, 1.5, the E_v and Γ_v are respectively equal to 2.70, 2.65, 2.60, 2.65 and 0.90, 1.50, 2.70, 4.80 mm. We can observe the same effect of the mass although the mold diameter and nature (PP) is different. Finally, for the $\varnothing$ = 3.3 cm samples (PS), the volume expansions are equal to 2.40 for a $^{3.3}{}_{0.27}F^{70}$ sample with $\varnothing/H$ = 5.4 and 2.80 for standard sample $^{3.3}{}_{1}F^{70}$ whereas the measured Γ_v are 0.80 mm and 3.70 mm.

The volume expansion is quite stable whatever the mass introduced is. This deduction can be extended to any diameter although we can suppose that using a mold diameter close to the pore diameter value itself will promote their coalescence because of the minimum free space. This result is in agreement with the relative proportion of the final solid network which is proportionally linked with the added mass.

However, for a same mold diameter, increase of the mass introduced induces a higher value of Γ_v, and this is the case for the three diameters used. Increase of the amount of foam network implies more water to evacuate for the same air/foam interface. Then the viscosity limit permitting coalescence control is achieved later. As a consequence, pore sizes are bigger. For a constant mass introduced inside the different molds ($^{5}{}_{1}F^{70}$ and $^{3.3}{}_{1}F^{70}$), it is the reverse: the air/foam interface is different for a constant water content to evacuate, so the pores are smaller when the diameter of the mold is larger. This can be correlated to drying of aqueous suspensions and drainage inside porous wet materials [22,23]. This confirms that gel formation is important at 70 °C, and it is possible to control the pore size by changing the mass of the foam and the air/foam surface. These experiments have been carried out at 55 °C and 23 °C too. The evolution of E_v and Γ_v are similar to those at 70 °C. However the importance of drying is reduced when the temperature decreases. As a consequence the addition of foam in a mold of constant diameter does not affect so much the pore size at 23 °C as gas production is not so rapid as it is at 70 °C.

To see the influence of both the exchange surface with air S_{air} and the exchange surface between the foam and the mold S_{tube} (foam in contact with the tube walls), for different molar quantities of foam introduced, on the final Γ_v of the foam, Fig. 9 represents the Γ_v values for all the samples synthesized at 70 °C as a function of the ratio n_{foam} (moles) over each surface exchange. The units of both vertical axes are the same for a better comparison. The ratio n/S_{air} is important for the drying aspect whereas n/S_{tube} represents the influence of the walls of the mold. This relates to mechanical and thermal effects. It is also possible to see the influence of one surface when the other is fixed. It is important to mention for understanding, that for a same value of Γ_v on this graph, the number of moles n is constant. When increasing n/S_{air}, Γ_v increases too with a strong dependence whereas it is possible to have a large range of Γ_v values for similar n/S_{tube} values.

3.5. Mechanical aspect

The standard mass of foam, m_0, is poured into two cylindrical molds with the same diameter (Φ = 3.3 cm) one made with polystyrene and the other made with polypropylene ($E_{polystyrene}$ = 3 GPa, $E_{polypropylene}$ = 1.5 GPa). Fig. 10 presents

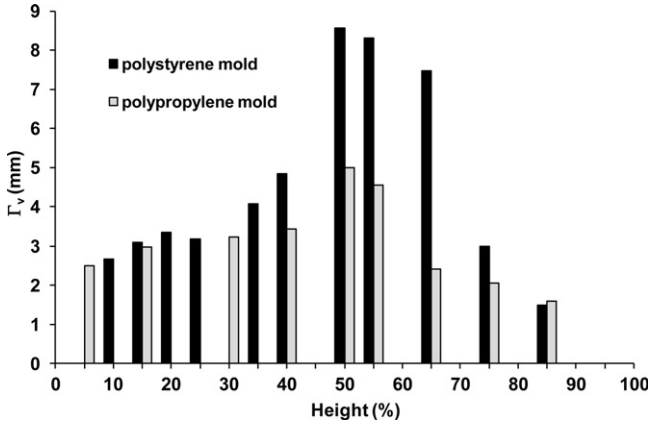

Fig. 10. Variation of Γ_v values for a $^{3.3}{}_{1}F^{70}$ sample at different heights for a mixture poured into a polystyrene (a) and polypropylene (b) mold.

the results at 70 °C of Γ_v at different heights for the two samples. The values of Γ_v are similar (∼3 mm) except at medium sample height where the pore sizes are significantly different. The pore sizes of the foam dried inside the less rigid mold is smaller, and the heterogeneity of pore sizes is attenuated. This could be due to a different surface roughness giving more opportunities for the bubbles to appear and then slip along the walls of the mold or deformation of the walls due to internal stresses, relaxing the foam.

4. Conclusion

This study showed that it was possible to control the porosity of a geopolymer foam without additives and for a constant chemical composition. The influence of processing parameters such as temperature, temperature cycles, the variation of surface exchange with air and the amount of mixture poured were tested. Whatever the experimental conditions, foam formation is a competition between the polycondensation reactions leading to the gel and the formation of hydrogen gas.

For constant temperature at 50 °C it is possible to synthesize a homogeneous foam sample with a $\Gamma_v = 1.5$ mm. Even if the synthesis is made at a lower temperature, it is still possible to take advantage of the drying effect and to control the porosity by changing the amount of foam and/or the surface exchange with air. The experiments based on the mass effect show that an increase of mixture induces higher values of Γ_v but does not affect the E_v. Furthermore, introduction of constant mass into molds of increasing diameter leads to a decrease of Γ_v.

Finally, two step temperature cycles can be used to control the pore size (Γ_v) and the homogeneity of this porous eco-material. A range of foams were made with a pore size Γ_v ranged from 0.6 to 1.5 mm. In future works, attention will be paid to the importance of the mold and its interaction with the mechanical behavior of the foam.

References

[1] K. Ishizaki, S. Komarneni, M. Nauko, Porous Materials: Process Technology and Applications, Kluwer Academic Publishers, London, 1998.
[2] J. Luyten, S. Mullens, F. Snijkers, A. Buekenhoudt, Pore architecture for a vast range of applications, in: Global Roadmap for Ceramics-ICC2 Proceedings, ISTEC-CNR, Verona, (2008), pp. 309–316.
[3] K.E. Pappacena, K.T. Faber, H. Wang, W.D. Porter, Thermal conductivity of porous silicon carbide derived from wood precursors, J. Am. Ceram. Soc. 90 (9) (2007) 2855–2862.
[4] E. Gregorova, W. Pabst, Z. Zivcova, Starch as a pore-forming and body-forming agent in ceramic technology, Starch 61 (9) (2009) 495–502.
[5] A.C. Pierre, Porous sol–gel ceramics, Ceram. Int. 23 (3) (1997) 229–238.
[6] P. Sepulveda, F.S. Ortega, M.D.M. Innocentini, V.C. Pandolfelli, Properties of highly porous hydroxyapatite obtained by the gel casting of foams, J. Am. Ceram. Soc. 83 (12) (2000) 3021–3024.
[7] X. Mao, S. Wang, S. Shimai, Porous ceramics with tri-modal pores prepared by foaming and starch consolidation, Ceram. Int. 34 (1) (2008) 107–112.
[8] V. Labiausse, Rhéologie non linéaire des mousses aqueuses, PhD Thesis, University of Marne la Vallée, 2004.
[9] C.J.W. Breward, The mathematics of foam, PhD Thesis, University of Oxford, 1999.
[10] M.A. Bos, T. Van Vliet, Interfacial rheological properties of adsorbed protein layers and surfactants: a review, Adv. Colloid Interface Sci. 91 (3) (2001) 437–471.
[11] L. Cheng, D. Mewes, A. Luke, Boiling phenomena with surfactants and polymeric additives: a state-of-the-art review, Int. J. Heat Mass Transfer 50 (13–14) (2007) 2744–2771.
[12] J. Davidovits, Geopolymer: Chemistry and Applications, 2nd edition, Geopolymer Institute, St. Quentin, France, 2008.
[13] P. Duxson, J.L. Provis, G.C. Lukey, J.S.J. Van Deventer, The role of inorganic polymer technology in the development of 'Green concrete', Cement Concrete Res. 37 (12) (2007) 1590–1597.
[14] E. Prud'homme, P. Michaud, E. Joussein, C. Peyratout, A. Smith, S. Rossignol, Consolidated geo-materials from sand or industrial waste, Ceram. Eng. Sci. Proc. 30 (2) (2010) 313–324.
[15] E. Prud'homme, P. Michaud, E. Joussein, C. Peyratout, A. Smith, S. Arrii-Clacens, J.M. Clacens, S. Rossignol, Silica fume as porogen agent in geo-materials at low temperature, J. Eur. Ceram. Soc. 30 (7) (2010) 1641–1648.
[16] M. Soustelle, Cinétique hétérogène vol 2: Mécanismes et lois cinétiques, Lavoisier Edition, Paris, 2006.
[17] S. Vincent-Bonnieu, Simulation et modélisation mutliéchelles de la rhéologie des mousses 2D, PhD Thesis, University of Marne la Vallée, 2006.
[18] C. Fritz, Transport de liquide et de particules dans un bord de plateau, PhD Thesis, University of Marne la Vallée, 2006.
[19] S.A. Koehler, H.A. Stone, M.P. Brenner, J. Eggers, Dynamics of foam drainage, Am. Phys. Soc. 58 (2) (1998) 2097–2106.
[20] R.D. Cadle, Particle Size Theory and Industrial Applications, Reinhold Publishing Corp., New York, 1965.
[21] L. Courthèoux, F. Popa, E. Gautron, S. Rossignol, C. Kappenstein, Platinum supported on doped alumina catalysts for propulsion applications. Xerogels versus aerogels, J. Non Cryst. Solids 350 (2004) 113–119.
[22] M. Mezhericher, A. Levy, I. Borde, Heat and mass transfer of single droplet/wet particle drying, Chem. Eng. Sci. 63 (1) (2008) 12–23.
[23] M. Prat, On the influence of pore shape, contact angle and film flows on drying of capillary porous media, Int. J. Heat Mass Transfer 50 (7–8) (2007) 1455–1468.